

Heat capacity measurements of petroleum fuels by modulated DSC

A. Zanier *, H.W. Jäckle

*Fuels & Lubricants Department of the Swiss Federal Laboratories for Materials Testing and Research
(EMPA), Überlandstrasse 129, 8600 Dübendorf, Switzerland*

Received 21 December 1995; accepted 29 March 1996

Abstract

In this work, the usefulness of modulated DSC (MDSC) for measuring the heat capacity of commercial hydrocarbon fuels is illustrated. Specifically, the reliability of the method is outlined by testing five liquid fuels of diverse composition and origin over a temperature range between -70°C and 70°C . The experiments were carried out using a DSC 2910 module from TA Instruments Inc., upgraded with the MDSC option. The samples were exposed to a cyclic heating profile which was generated by a linear heating rate of $2^{\circ}\text{C min}^{-1}$ while simultaneously superimposing a sinusoidally varying time-temperature wave with an amplitude of $\pm 0.5^{\circ}\text{C}$ and a period of 100 s.

On the basis of these measurements, MDSC proved to be a valuable technique with which to measure directly the heat capacity of hydrocarbon fuels. Moreover, the ability of MDSC to measure heat capacity with great accuracy and precision offers a powerful approach for studying the effects of compositional differences on heat capacity.

Keywords: Fuels; Heat capacity; MDSC

1. Introduction

The heat capacities of petroleum hydrocarbons and their mixtures are of practical importance in engineering work associated with petroleum refinery operations and related processes. Not only does the design of plant equipment require a knowledge of heat capacity data over wide ranges in temperature, but these data are also

* Corresponding author.

helpful when prolonged storage or low temperature operability are considered. Heat capacity can then be used in the evaluation of other basic thermodynamic properties of the fuel.

Computation of the heat capacity from theoretical considerations or relating it to any other single physical property have proven unreliable for petroleum fractions except for limited applications in the liquid range [1, 2]. Consistent experimental heat capacity data for petroleum fuels are quite limited, and even when available cover small temperature ranges for the most part. Whether potential differences in the composition of the fuels result in significant heat capacity differences is often not predictable but must be confirmed by testing before use.

In recent years, differential scanning calorimetry (DSC) has been successfully used for the determination of the specific heat capacity of hydrocarbon mixtures [3]. However, it requires multiple experiments and considerable operator skill to obtain results with acceptable accuracy and precision. One means of obtaining accurate heat capacity data more directly is through the use of modulated DSC (MDSC), which is a recently developed extension to conventional DSC [4–6].

It is the object of this paper to show that MDSC analysis can easily be used to measure the heat capacity of petroleum fuels. The test procedure developed can assist the chemist in characterizing petroleum products.

2. Principle of the measurement

In modulated DSC the same heat flux DSC cell arrangement is used as in conventional DSC, but a different heating profile is applied by the furnace to the sample and reference. Specifically, a sinusoidal temperature modulation (oscillation) is overlaid on the traditional linear heating ramp to yield a cyclic heating profile. The temperature increases at a rate which is sometimes faster, sometimes slower, than the underlying heating rate. The actual variations in heating rate obtained depend on three experimental variables: the underlying heating rate, the amplitude of modulation, and the frequency of modulation [6]. The combination of the underlying heating rate with the more rapid instantaneous heating rate results in improved sensitivity without loss of resolution. In the present investigation, the selected underlying heating rate, modulation amplitude, and modulation period resulted in an instantaneous heating rate varying between $+3.9$ and $+0.1^\circ\text{C min}^{-1}$ (Fig. 1).

Separating the resultant complex calorimetric response using a discrete Fourier transformation algorithm provides not only the total heat flow obtained from conventional DSC, but also separates that total heat flow into its heat-capacity-related (reversing) and kinetic (non-reversing) components [7–9].

In MDSC, the heat flow values during a scan are converted directly to heat capacity values at the indicated temperature by dividing the modulated heat flow amplitude by the modulated heating rate amplitude. Fig. 2 gives the results expressed in this fashion for an experiment on *n*-dodecane. It is apparent that if no physical transformations occur in the sample the real heat capacities can be easily determined by calibrating this cyclic heat capacity signal.

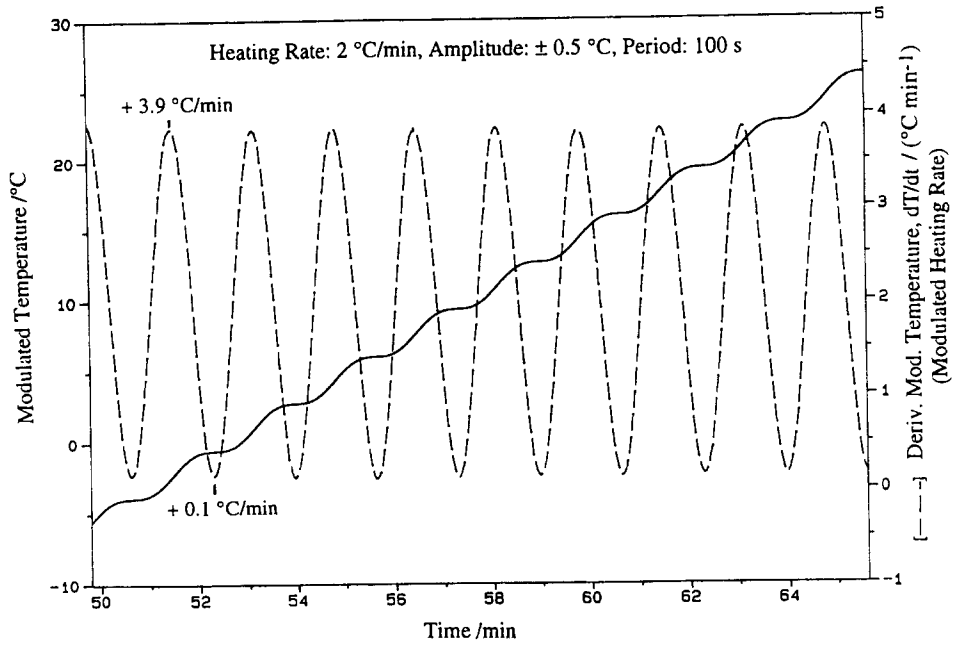


Fig. 1. MDSC heating profile (cyclic heating only).

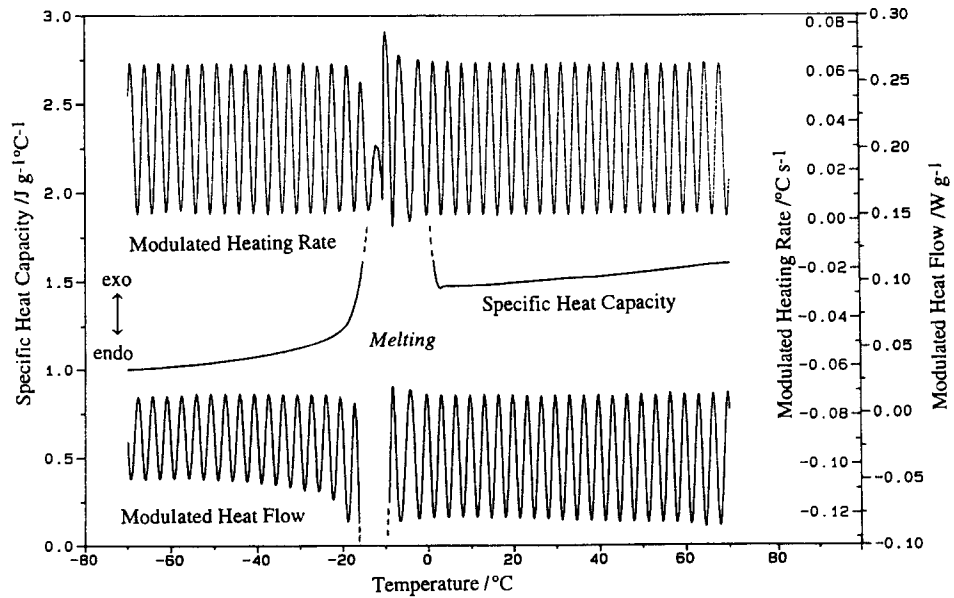


Fig. 2. Heat capacity from MDSC raw signals (experiment on *n*-dodecane).

Using MDSC for heat capacity measurements, a baseline correction is not necessarily required providing the heat capacity imbalance of the cell is very small and the weights of the sample and reference pans are carefully matched [9].

3. Experimental

3.1. The samples

Petroleum fuels are mixtures of paraffin, naphthenic and aromatic hydrocarbons, plus organic sulphur, oxygen, and nitrogen compounds that were not removed by refining. They are specified according to the classifications adopted by standard associations and institutions as the result of a compromise between desirable performance characteristics in the product and the ability of the refiner to make such a product from the crude oil at hand. Routine laboratory tests methods are universally used to check the defined requirements.

For the investigation, the following five commercial fuels were examined:

Sample 0170: unleaded automotive gasoline conforming to European Standard EN 228;

Sample 1508: aviation turbine fuel “Jet A-1”;

Sample 1610: a special grade of fuel oil for automotive diesel engines conforming to European Standard EN 590, class 2;

Sample 2005: fuel oil for automotive diesel engines conforming to European Standard EN 590, class 0;

Sample 7962: cracked gas oil for use in domestic or small industrial burners satisfying the specifications DIN 51603-1.

These samples were selected as a reflection of the diversity of conventional fuels and analyzed prior to the thermoanalytical work. The more pertinent physical and chemical properties of these fuels, arranged in order of increasing density, are summarized in Table 1.

3.2. Instrumentation and procedure

The experiments were performed using a DSC 2910 module from TA Instruments Inc., upgraded with the MDSC option. A complete description of this device is given elsewhere [7].

A great deal of attention was given to finding the conditions that yielded an optimum of reproducibility by adopting a simplified measurement technique without the conventional yet time-consuming additional run with an empty crucible to correct for baseline curvature. This was possible because the heat capacity imbalance of the cell was less than 1 mJ K^{-1} . However, before starting measurements, the DSC module was adjusted by software for heat flow signal zero to lie between 0 and -0.5 mW , and the baseline drift to be less than 0.1 mW over the temperature range of interest.

A heating rate of 2°C min^{-1} , an amplitude of modulation of $\pm 0.5^\circ\text{C}$ and a period of 100 s were used throughout this investigation. Hermetic aluminium crucibles of $40 \mu\text{l}$

Table 1
Physical and chemical properties of the selected fuels

Property	Units	Method	Gasoline Sample 0170	Jet fuel Sample 1508	Diesel oil Sample 1610	Diesel oil Sample 2005	Heating oil Sample 7962
Density at 15°C	kg m ⁻³	ASTM D 4052	725.8	801.4	816.3	830.3	846.5
Cloud point	°C	ISO 3015	—	—	-32	-11	±0
Pour point	°C	ISO 3016	—	—	-36	-30	-21
Freezing point	°C	ASTM D 2386	—	-54.5	—	—	—
Viscosity at 40°C	mm ² s ⁻¹	ISO 3104	—	1.24	2.23	2.32	3.17
Micro carbon residue	mass%	ASTM D 4530	—	—	0.01	0.01	0.07
Carbon	mass%	ASTM D 5291	85.90	85.40	85.43	85.74	86.35
Hydrogen	mass%	ASTM D 5291	14.10	14.35	14.43	14.02	13.50
Sulphur	mass%	ASTM D 3453	0.005	0.013	0.001	0.024	0.145
Nitrogen	mg kg ⁻¹	ASTM D 4629	4	6	2	83	198
Distillation at 101.3 kPa		ASTM D 86					
initial boiling point	°C		42	156	199	167	178
10 vol. % recovered at	°C		52	174	220	203	215
30 vol. % recovered at	°C		70	185	235	232	254
50 vol. % recovered at	°C		95	196	251	256	285
70 vol. % recovered at	°C		113	209	271	282	332
90 vol. % recovered at	°C		156	228	288	319	354
end point	°C		181	249	312	351	379

volume available from Mettler Instruments were employed. The combined mass of pans and lids was always about 49 mg and matched on the sample and reference sides to within ± 0.10 mg. They were cleaned in diethyl ether prior to use. Sample masses were approximately 20 mg for both calibration and measurements. An empty sealed crucible was used as a reference. As for motor gasoline, which develops a considerable vapour pressure at ambient temperature, the fuel had to be cooled significantly before encapsulating.

The measurements were carried out using liquid nitrogen coolant and helium purge gas with a flow rate of 40 ml min^{-1} . Helium was chosen because of its comparatively high thermal conductivity so as to obtain maximum temperature uniformity across the test specimen, thereby enhancing the accuracy of the measurement.

The temperature calibration was carried out using the onsets of the transition peaks for *n*-octane, 3-pentanone, *n*-dodecane and stearic acid (melting points, -56.8 , -39.0 , -9.6 and 70.0°C , respectively). The employed calibrants were all of analytical reagent grade.

Reference materials (puriss. standard for GC) were *n*-heptane for heat capacity calibration in the liquid temperature range and *n*-dodecane for calibration over the temperature range of the solid phase. Both compounds have physical properties similar to the samples being investigated and their heat capacities are known accurately from the literature [10, 11]. Heat capacity calibration was made by running the reference materials under the same experimental conditions as would be used for the fuel samples and comparing the determined specific heat capacities ($C_{p,\text{obs}}$) with the literature values ($C_{p,\text{lit}}$) at the temperatures of interest. The resulting calibration coefficient (K) was then used to correct the $C_{p,\text{obs}}$ of each sample at that temperature, except for the temperature intervals in which a phase transition occurred and a second phase was present. The values obtained were taken as the experimental specific heat capacities of the sample ($C_{p,\text{exp}}$).

The samples were quickly cooled to the initial temperature (-80°C , except for sample 1508, which was cooled to -50°C), without collecting data. After giving the entire system time to stabilize by being held isothermally for 10 min at this temperature with the selected modulation period and temperature amplitude, the data storage was turned on and with continued liquid nitrogen feeding the underlying heating started. The heating was stopped at the desired final temperature ($+70^\circ\text{C}$, except for sample 0170, $+40^\circ\text{C}$). When the cell had cooled to room temperature, the sample pan was reweighed to ensure zero weight loss from vaporization.

Since the enthalpy of vaporizing contributes significantly to the apparent heat capacity of the condensed sample, the tests were not extended above 70°C . At least five runs were carried out on different samples of each fuel, and the data collected were averaged and then smoothed graphically.

4. Results and discussion

The final results of the measurements in the solid and liquid phase are plotted in Fig. 3 and given for selected temperatures between -70 and 70°C , in Table 2. It is

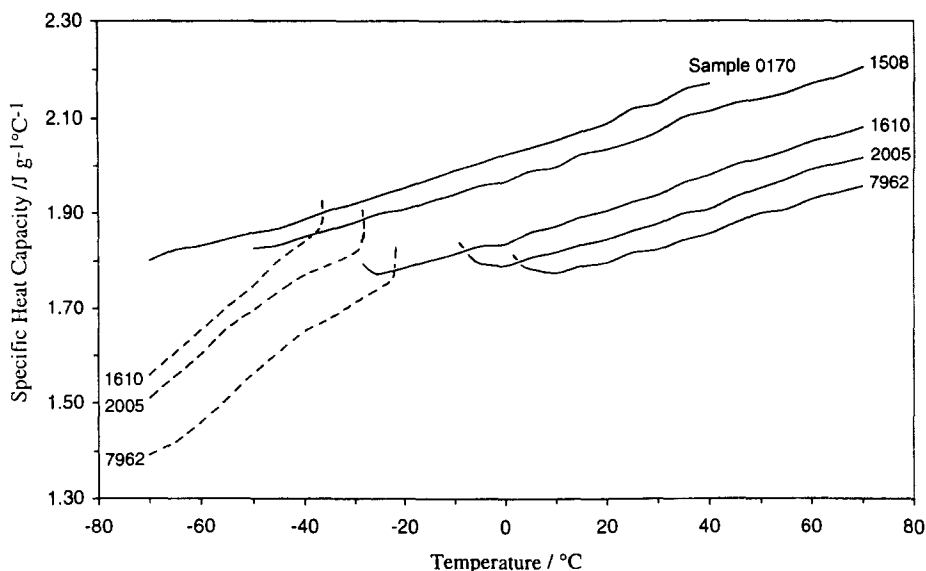


Fig. 3. Specific heat capacities of the selected samples. The dashed curves represent the data of the solid phase.

apparent in Fig. 3 that the heat capacity of the selected fuels rises linearly with an increase in temperature both in the liquid and solid region. The difference in heat capacity among the fuels is due to the differences in chemical composition. In the normal liquid range, the heat capacity of the fuels is generally a function of density and of the nature of the stock [12]. As the paraffinic nature of the stock diminishes, the heat capacity tends to decrease. The higher boiling fractions of petroleum stocks tend to be less paraffinic than the low boiling fractions and have higher values of density. Therefore, sample 0170 (motor gasoline) has the highest heat capacity, and sample 7962 (heating oil) the lowest of the selected fuels. This relationship cannot be generalized to all fuels, however.

Samples 1610, 2005 and 7962 underwent a solid to liquid phase transition within the operating temperature range. In each case, a marked increase in slope occurs due to the influence of the endothermic event on the cyclic heat capacity signal. It is difficult to estimate quantitatively the amount of excess heat capacity above the “normal” value, particularly since in this region heat capacity data were not reproducible within the normal precision of the measurements.

For these samples, a stronger temperature dependence of the heat capacity heat in the solid phase was observed than in the liquid phase in the range considered. In the liquid region, their heat capacity is larger than in the solid, as is usually observed in many hydrocarbon fuels. An exception are the values in the pre-melting region for samples 1610 and 2005 which are significantly higher than those in the liquid phase just above the melting end. This is probably connected with some type of “pre-rotation” in the solid and reflects the changes in internal free volume available for molecular motion

Table 2
Calibration coefficients and experimental heat capacities (in $\text{J g}^{-1} \text{K}^{-1}$) of the tested fuels

$T/^\circ\text{C}$	<i>n</i> -Heptane		K_{hep}	<i>n</i> -Dodecane		K_{dod}	Sample 0170		Sample 1508		Sample 1610		Sample 2005		Sample 7962	
	$C_{p,\text{obs}}$	$C_{p,\text{lit}}$ [10]		$C_{p,\text{obs}}$	$C_{p,\text{lit}}$ [11]		$C_{p,\text{exp}}$	$C_{p,\text{exp}}$	$C_{p,\text{exp}}$	$C_{p,\text{exp}}$	$C_{p,\text{exp}}$	$C_{p,\text{exp}}$	$C_{p,\text{exp}}$	$C_{p,\text{exp}}$	$C_{p,\text{exp}}$	
-70	1.477	2.009	1.360	1.002	1.319	1.316	1.800	1.559	—	1.509	1.392					
-65	1.465	2.012	1.373	1.010	1.345	1.332	1.823	1.605	—	1.509	1.419					
-60	1.451	2.015	1.389	1.021	1.373	1.345	1.832	1.653	phase transition	1.602	1.458					
-55	1.445	2.021	1.399	1.031	1.401	1.359	1.846	1.703	phase transition	1.657	1.509					
-50	1.441	2.028	1.407	1.044	1.432	1.371	1.859	1.747	1.826	1.696	1.562					
-45	1.436	2.036	1.418	1.060	1.463	1.380	1.868	1.801	1.833	1.735	1.607					
-40	1.431	2.046	1.430	1.077	1.497	1.390	1.887	1.841	1.851	1.770	1.651					
-35	1.436	2.056	1.432	1.102	1.532	1.390	1.906	phase transition	1.866	1.791	1.678					
-30	1.440	2.068	1.436	1.126	1.571	1.395	1.921	phase transition	1.881	1.818	1.713					
-25	1.442	2.080	1.442	1.163	1.611	1.386	1.937	1.773	1.900	↓	1.743					
-20	1.447	2.094	1.447	1.222	1.656	1.355	1.953	1.785	1.908	phase transition	↓					
-15	1.456	2.108	1.448	1.460	1.702	—	1.971	1.801	1.925	phase transition	↓					
-10	1.464	2.122	1.450	phase transition	phase transition	—	1.990	1.815	1.940	phase transition	↓					
-5	1.471	2.138	1.453	1.470	2.148	—	2.006	1.831	1.957	↓	↓					
±0	1.485	2.154	1.451	1.470	2.148	—	2.025	1.837	1.967	1.795	↓					
5	1.491	2.171	1.456	1.475	2.157	—	2.039	1.861	1.989	1.790	↓					
10	1.504	2.189	1.455	1.479	2.168	—	2.055	1.861	1.998	1.807	1.784					
15	1.513	2.206	1.458	1.484	2.180	—	2.084	1.873	2.025	1.819	1.775					
20	1.528	2.224	1.456	1.495	2.194	—	2.090	1.893	2.037	1.834	1.789					
25	1.540	2.243	1.456	1.503	2.208	—	2.119	1.906	2.052	1.846	1.796					
30	1.556	2.262	1.454	1.514	2.223	—	2.130	1.924	2.073	1.864	1.817					
35	1.561	2.281	1.461	1.524	2.238	—	2.159	1.938	2.103	1.878	1.824					
40	1.578	2.300	1.458	1.533	2.254	—	2.171	1.964	2.114	1.899	1.844					
45	1.588	2.302	1.461	1.546	2.270	—	—	1.980	2.114	1.908	1.857					
50	1.603	2.341	1.460	1.555	—	—	—	2.002	2.130	1.933	1.879					
55	1.619	2.361	1.458	1.566	—	—	—	2.015	2.139	1.952	1.900					
60	1.632	2.382	1.460	1.576	—	—	—	2.032	2.151	1.970	1.928					
65	1.649	2.404	1.458	1.588	—	—	—	2.052	2.171	1.991	1.943					
70	1.666	2.426	1.456	1.604	—	—	—	2.066	2.185	2.004	1.943					
								2.082	2.206	2.018	1.957					

[11]. These findings lend support to the assumption that there are *n*-paraffin molecules which tend to rotate about their longitudinal axes at temperatures below their melting points. Unlike cracked fractions, such straight-run distillates contain considerable amounts of low freezing *n*-paraffins. The pre-melting contribution to the recorded apparent heat capacity appears to be greater for sample 1610. Its narrower hydrocarbon fraction may ensure a better transport of pre-melted material by capillaries between the borders of more uniform crystallites. Similar phenomena have been reported in investigations on pure paraffin hydrocarbons [13].

The error is estimated to be <2% in the liquid phase below +30°C, and <3% in the solid phase and in the liquid phase between +30 and +70°C, where the results are less reliable owing to the uncertainty arising from the increasing vapour pressure. Moreover, because the actual internal volume of a given crucible was not known exactly, no corrections were made for the enthalpy involved in vaporizing small amounts of samples into the vapour space of the sealed crucibles. Nevertheless, except for sample 0170 (motor gasoline), no anomalous increase in the heat capacity curve was observed up to +70°C.

Despite the specific character of the fuels investigated, which makes a direct comparison with the literature data not always possible, the findings are entirely consistent with those reported in previous studies in which conventional DSC was employed [3,14].

5. Conclusions

The results obtained in this research for the selected fuels provide convincing evidence that MDSC is a suitable technique for easy measurement of the heat capacity of fuels. Once the optimum operation conditions have been established, the heat capacity can be determined directly with great accuracy and precision, within an acceptable period of time.

These findings suggest that future experiments should also include heat capacity measurements at temperatures covering the phase transition region. This could be accomplished by measuring the heat capacity at practically isothermal conditions (isothermal except for temperature modulation) at selected temperatures over the two-phase region.

Although further work must be carried out, there are some encouraging indications that MDSC will ultimately improve the detection limit for changes in heat capacity, thus enabling, for example, the detection of additives or degradation products of fuels.

References

- [1] Annual Book of ASTM Standards, Calculation of Liquid Heat Capacity of Petroleum Distillate Fuels, Vol. 05.02, D 2890, 1992.
- [2] S.T. Hadden, *Hydrocarbon Processing*, 45 (1966) 137.
- [3] W.V. Steele, R.D. Chirico, National Institute for Petroleum and Energy Research, Report No. 395, Bartlesville OK, 1989.

- [4] S.R. Sauerbrunn, B.S. Crowe and M. Reading, *Polym. Mater. Sci. Eng.*, 68 (1993) 269.
- [5] P.S. Gill, S.R. Sauerbrunn and M. Reading, *J. Therm. Anal.*, 40 (1993) 931.
- [6] M. Reading, *Trends Polym. Sci.*, 1(8) (1993) 248.
- [7] *Modulated DSC Theory, Application Brief No. TA 74*, TA Instruments, New Castle, DE, 1994.
- [8] M. Reading, D. Elliot and V.L. Hill, *J. Therm. Anal.*, 40 (1993) 949.
- [9] M. Reading, A. Luget and R. Wilson, *Thermochim. Acta*, 238 (1994) 295.
- [10] C. Dafoe, C. Ginning and G. Furukawa, *J. Am. Chem. Soc.*, 75 (1953) 522.
- [11] H.L. Finke, M.E. Gross, G. Waddington and H.M. Huffman, *J. Am. Chem. Soc.*, 76 (1954) 333.
- [12] K.M. Watson and E.F. Nelson, *Ind. Eng. Chem.*, 25 (1933) 880.
- [13] J.F. Messerly, G.B. Guthrie, S.S. Todd and H.L. Finke, *J. Chem. Eng. Data*, 12 (1967) 338.
- [14] J.G. Zimmerman, U.S. NTIS, Rep. AD-A039655, 1977.